

## Conformational studies of antisense DNA by PFG NMR

Xueyong Yang<sup>a</sup>, Yogesh S. Sanghvi<sup>b</sup> and Xiaolian Gao<sup>a,\*</sup>

<sup>a</sup>Department of Chemistry, University of Houston, Houston, TX 77204-5641, U.S.A.

<sup>b</sup>Isis Pharmaceuticals, Medicinal Chemistry Department, 2292 Faraday Avenue, Carlsbad, CA 92008, U.S.A.

Received 8 May 1997

Accepted 11 July 1997

**Keywords:** Antisense oligonucleotides; Backbone modification; Diffusion constant; Hairpin conformation; Pulsed field gradient NMR

### Summary

Pulsed field gradient diffusion constant measurements were used to resolve the ambiguity in determining the conformational states of single-stranded DNA dodecanucleotides (d1s, d4s and d5s). For d1s and d5s, because of the spectral symmetry conventional NMR analyses cannot differentiate whether they are hairpins or homo-duplexes. However, the diffusion constants of these sequences at 300 K are 1.4 times greater than those of the comparison complementary duplexes. This result agrees well with what is expected for  $D_{\text{hairpin}}/D_{\text{duplex}}$  based on classic liquid-phase translational diffusion models and the Einstein–Stokes equation, confirming that d1s and d5s form hairpins. d4s did not show a structured spectral pattern, but its diffusion constant measurement suggests that this sequence may not be a random coil. The DNA sequences studied contain chemically modified backbone linkages and are potential antisense agents for gene regulation. The knowledge of their diffusion constants, in combination with conventional NMR analysis and other biophysical spectroscopic measurements, provides new insights into the relationships of chemical structure and conformational preference of antisense oligonucleotides and their analogs.

### Introduction

Antisense gene regulation involves oligodeoxyribonucleotides, oligoribonucleotides or their analogs (hereafter called oligonucleotides in general, unless otherwise specified) interacting with mRNA or DNA at specific sites (Zamecnik and Stephenson, 1978; Crooke, 1992; Agrawal and Iyer, 1995; Cole-Strauss et al., 1996; Matteucci and Wagner, 1996; Stein, 1996; Sanghvi, 1997). To achieve specific and high-affinity binding, the properties of single-stranded antisense oligonucleotides should be such that complex formation with target strands is energetically favored over formation of intramolecular secondary structures. The driving force for hybridization to form a duplex will likely be reduced if an intermediate, single-stranded structure exists, i.e. if antisense oligonucleotides assume preorganized conformations (Vesnaver and Breslauer, 1991). In our investigation of antisense oligonucleotides containing various modified backbone linkages (Fig. 1) (Gao et al., 1992; Veal et al., 1993; Gao and Jeffs, 1994a,b; Veal and Brown, 1995; Cross et al., 1997; Rice and Gao,

1997), we began to ask questions about the effects of these backbone linkers on the conformation and conformational flexibility of the single-stranded sequences. For the reasons discussed above, these properties should greatly influence the formation of single-stranded structures and the hybridization of antisense sequences with target mRNA or DNA sequences. Furthermore, the conformational preferences of the single-stranded sequences should correlate with the fitness of the antisense strand in helices and the stability of the resultant helices. In the systems studied, the modified backbone linkers are incorporated into the d[C<sub>1</sub>G<sub>2</sub>C<sub>3</sub>G<sub>4</sub>T<sub>5</sub>T<sub>6</sub>T<sub>7</sub>T<sub>8</sub>G<sub>9</sub>C<sub>10</sub>G<sub>11</sub>C<sub>12</sub>] strand, which is hybridized with either a DNA or an RNA strand with a natural phosphodiester backbone to form a complementary duplex. The detailed characterization of six such duplexes and the high-resolution structure of the RNA•DNA hybrid duplex containing a T<sub>6</sub>-SCH<sub>2</sub>O-T<sub>7</sub> (3'-thioformacetal) have been reported (Gao et al., 1992; Veal et al., 1993; Gao and Jeffs, 1994a,b; Veal and Brown, 1995; Cross et al., 1997; Rice and Gao, 1997). When the modified sequences (see examples in Fig. 1) were examined as

\*To whom correspondence should be addressed.

Supplementary Material available from the authors: three figures, containing <sup>1</sup>H spectra recorded in 90% H<sub>2</sub>O/10% D<sub>2</sub>O and in D<sub>2</sub>O, and a stacked plot of the LED-STE-PFG experiments.

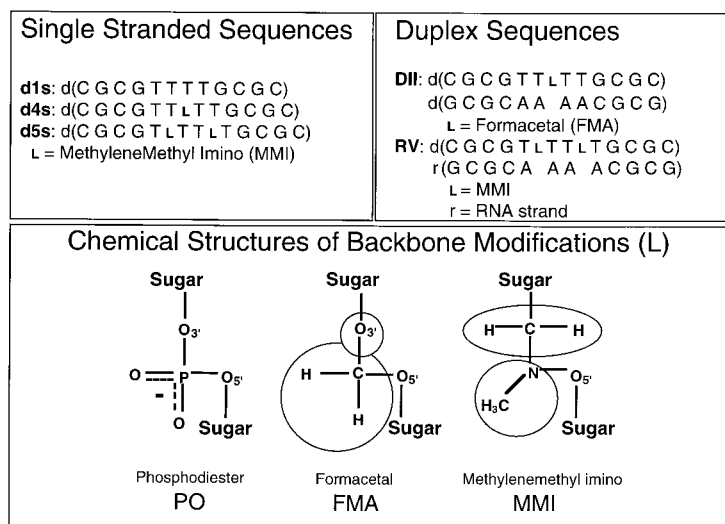


Fig. 1. Oligonucleotide sequences and chemical structures of the backbone linkage modifications used in this study.

single strands by temperature-dependent UV measurements, they all displayed broad, undefined transitions of similar appearance. The hyperchromicity of these melting curves was less than 5% (our unpublished results), much lower than the 10–15% normally observed for the melting of helical nucleic acids. These UV results seem to indicate nonspecific intra- or interstrand associations, which are general behaviors of random single-stranded sequences. However, NMR spectra of the same set of sequences demonstrate interesting features (Fig. S1, supplementary material). The unmodified d[CGCGTTTTGCGC] (d1s) and the modified d[CGCGTTLTTGCGC] (d5s, L=MMI, the methylenemethyl imino linker, Fig. 1) (Vasseur et al., 1992) displayed Watson–Crick hydrogen bonded G imino protons at the 13 ppm region at a temperature as high as 318 K (Figs. S1A and C). In contrast, the mono-MMI modified sequence, d[CGCGTTLTTGCGC] (d4s), containing a single MMI linker between the T6 and T7 residues, existed in a hydrogen bonded form only at very low temperatures (<278 K). At room temperature, the exchangeable  $^1\text{H}$  spectrum of this sequence is structurally featureless (Fig. S1B) and the nonexchangeable  $^1\text{H}$  spectrum displayed somewhat reduced chemical shift dispersions (Fig. S2). These results have motivated us to pursue the experiments reported here.

It is tempting to believe that the presence of base paired G imino protons in single-stranded d1s and d5s is due to the formation of hairpins as shown in Fig. 2. This would allow us to correlate NMR data with the structural and dynamical functions of various backbone linkers in the oligonucleotides studied. There has been ample literature information on the characterization of DNA hairpin formation and their structures (Hilbers et al., 1985; Senior et al., 1986; Chattopadhyaya et al., 1990; Ippel et al., 1995; Varani, 1995). While many of these did not demonstrate the verification of hairpin versus duplex formation,

hairpin formation by a self-complementary strand can be confirmed by the presence of non-Watson–Crick base paired imino proton resonances at the 10–11 ppm region (Patel et al., 1987). Sometimes, oligonucleotides containing two complementary sequences linked by 2–4 loop residues (palindrome sequences), such as a string of T residues, are involved (Williamson and Boxer, 1989a,b). This type of sequence is assumed to prefer a hairpin form to a duplex form due to favorable entropy contributions. Several experimental methods have been applied to characterize hairpin formation. For instance, hairpin formation by a dodecamer sequence was confirmed by the demonstration of a shorter rotational correlation time than what was predicted for a duplex using depolarized dynamic light scattering (Eimer et al., 1990). In some cases hairpin formation was concluded based on the concentration independence of UV melting profiles, even though UV experiments were conducted at much lower concentrations. The sequences used in our studies are neither complementary strands nor palindrome types. These sequences possibly can form hairpins or homo-duplexes in a staggered alignment (Fig. 2). UV measurements of these single-stranded sequences demonstrated that their melting

#### A. Homo-Duplex



#### B. Hairpin

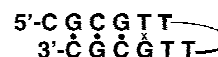


Fig. 2. The two possible conformations for single-stranded sequences: (A) the homo-duplex; and (B) the hairpin form. The filled circles and the crosses indicate Watson–Crick and mismatched base pairs, respectively. The base pair alignment was derived from detailed 1D and 2D NMR spectral analysis (Yang et al., manuscript in preparation).

profiles were unchanged when sample concentrations were varied sevenfold. However, since the NMR experiments were undertaken at concentrations 50–100 times that of the UV experiments, a direct assessment of the conformational state of these sequences is vital to our interpretation of the NMR data. Thus, the experiments discussed in this paper were to resolve the ambiguity arising from the fact that two possible forms of sequence folding, i.e. either the antiparallel homo-duplex or the hairpin (Fig. 2), would fit the observed NMR results for d1s and d5s.

In searching for NMR methods of identifying hairpin versus duplex forms, the pulsed field gradient (PFG) experiments measuring self-diffusion constants (Stejskal and Tanner, 1965; Gibbs and Johnson, 1991), attracted our attention. These experiments measure physicochemical parameters which are sensitive to the size and shape of molecules and are exemplary of the versatile applications of PFG, which have greatly widened and enhanced the role of NMR spectroscopy in dealing with small or large molecules (Stejskal and Tanner, 1965; Bax et al., 1980; Hurd, 1990; Gibbs and Johnson, 1991; Kay et al., 1992; Ruiz-Cabello et al., 1992; Altieri et al., 1995; Barjat et al., 1995; Lin and Larive, 1995; McCain, 1995; Antalek and Windig, 1996; Gozansky and Gorenstein, 1996; Senthil and Chandrakumar, 1996; Ilyina et al. 1997). In comparison with other biophysical measurements of diffusion constants ( $D_T$ 's), the advantages of the NMR approach are that the obtained information can be directly correlated with other NMR experiments and there is no need for additional equipment or alternation in sample preparation. Several well-characterized proteins, such as lysozyme, BPTI and ubiquitin, have been used to demonstrate the utility of  $D_T$  measurements in studying oligomerization of proteins (Altieri et al., 1995; Lin and Larive, 1995; Ilyina et al., 1997). The  $D_T$  values of these proteins measured by PFG NMR are close to those obtained from bioanalytical methods, such as light scattering experiments, and, more importantly, these  $D_T$  measurements are shown to be a reliable means for examination of oligomerization states of proteins. These experiments were performed under comparable conditions and demonstrated that the dimerization of a protein reduces  $D_T$  by ~29% or  $D_{T,monomer}/D_{T,dimer} \sim 1.4$ . We reasoned that these experiments should be applicable to the oligonucleotides shown in Fig. 1. The formation of a hairpin or a homo-duplex (the coexistence of the two states was not observed; Yang et al., manuscript in preparation) should be distinguishable from their  $D_T$  comparisons.

In this paper, we report the  $D_T$  measurements of single-stranded DNA sequences, d1s, d4s and d5s, by LED-STE-PFG NMR (LED: longitudinal eddy-current delay or longitudinal encode-decode; STE: stimulated echo) (Gibbs and Johnson, 1991). These results are compared with those of related duplexes RV (which is an RNA•DNA duplex directly related to d5s) and DII of the same chain length (Fig. 1). These comparisons provide critical

information that allows us to address the questions concerning the association and the folding states of the single-stranded antisense DNA sequences and a basis for comparison of the effects of backbone modifications on the formation of single-stranded structures.

## Materials and Methods

DNA sequences CGCGTTTTGCGC (d1s, 1.8  $\mu$ mol), CGCGTTLTTGCGC (d4s, 1.7  $\mu$ mol) and CGCGTLTTLTGCGC (d5s, 1.3  $\mu$ mol) ( $L = \text{MMI}$ , Fig. 1), the RNA•DNA hybrid duplex (RV, 1.1  $\mu$ mol in duplex) containing d5s and the complementary RNA strand, and the DNA•DNA duplex (DII, 1.5  $\mu$ mol in duplex) containing d2s (similar to d4s, but  $L = \text{formacetal}$ ) and the complementary DNA strand have been used in this study. Except for the backbone modified sequences, all DNA and RNA strands were synthesized using a Cruachem PS250 synthesizer as reported previously (Rice and Gao, 1997). The MMI-containing d4s and d5s were prepared by Isis Pharmaceuticals Inc. according to reported procedures (Vasseur et al., 1992). Final NMR samples were in a  $D_2O$  solution containing 0.1 M sodium chloride, 10 mM sodium phosphate and 0.1 mM disodium ethylenediaminetetraacetic acid (EDTA), at pH ~ 6.3. A hen egg white lysozyme sample (a gift from Dr. Bax, NIH), 10 mg dissolved in 1 ml of  $D_2O$ , was prepared for calibration of gradient field strength (vide infra).

NMR experiments were performed on a Bruker AMX-II 600 MHz spectrometer equipped with a z-gradient system (B-GB 30, maximum 30 G/cm). Proton resonances of the oligonucleotides studied have been assigned based on the analyses of their 1D and 2D NMR spectra (Gao et al., 1992; Yang et al., manuscript in preparation). In this work, each of the 1D experiments was collected with a 5.1 kHz spectral width and 4–8K complex data points to give a digital resolution of 1.03 Hz/point or better. Proton chemical shifts were referenced relative to the HOD resonance (4.68 ppm at 300 K). Nonselective  $T_1$  and  $T_2$  (the longitudinal and transverse relaxation times) were estimated for the d1s strand and the RV duplex at 300 K according to procedures described in the literature (Harris, 1986) for validation of the conditions  $T_1 \gg T_2 \gg \delta$  ( $\delta$  is the gradient duration).

$D_T$ 's were measured at 300 K. This temperature was selected based on the proper balance of several factors, such as the presence of the conformational states, the diffusion and the relaxation behavior of the oligonucleotides studied. The LED-STE-PFG pulse sequence was used (Gibbs and Johnson, 1991). The pulse sequence consists of a  $90^\circ\text{-}\tau\text{-}90^\circ\text{-}T\text{-}90^\circ\text{-}\tau$  echo (STE echo,  $T$  is a delay time) and a  $90^\circ\text{-}T_e\text{-}90^\circ$  longitudinal eddy-current delay. A pair of sine z-gradient pulses is applied at the beginning of  $\tau$  delays and separated by  $\Delta\text{-}\delta$  ( $\delta$  is the duration of the gradient pulse and  $\Delta$  is the diffusion delay time used in  $D_T$

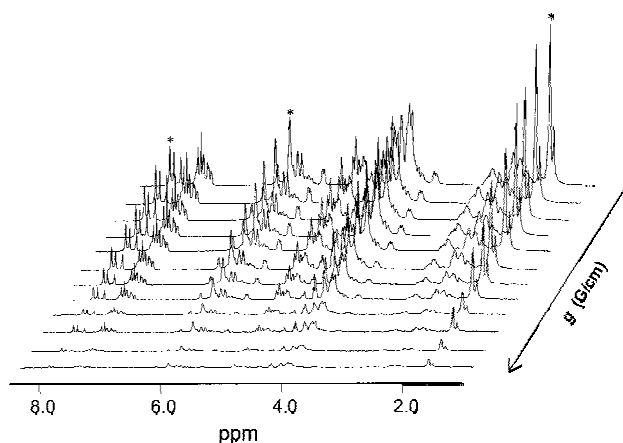


Fig. 3. Representative stacked plot of the LED-STE-PFG experiments for measurement of diffusion constants. The spectra of d1s recorded at 300 K are displayed in order of decreasing gradient field strength (from front to back). \* indicates resonances, the intensities of which were used to derive diffusion constants.

calculations). Typical experimental values used are  $\tau = 8.3$  ms,  $\delta = 5\text{--}8$  ms,  $\Delta = 132.4\text{--}158.3$  ms ( $\Delta = T + \tau$ ),  $T_e = 20$  ms and the strength of the gradient pulses,  $g$ , varied from 5% to 100% of 30 G/cm. A longer  $T_e$  delay (100 ms) did not seem to affect the decay rate of signal intensities. These experiments measured the modulation of the amplitude of nuclear spin echo by gradual change in pulsed gradient field strength (Hahn, 1950; Carr and Purcell, 1954; Stejskal and Tanner, 1965). If magnetic field inhomogeneity is negligible and the PFG pulse duration  $\delta$  is sufficiently short and much less than  $T_1$ , the reduction in spin echo amplitude follows the relationship

$$\ln(A') = -(\gamma\delta g)^2(\Delta - \delta/3)D_T + \ln(A_0) \quad (1)$$

where  $A'$  and  $A_0$  are measured peak intensities with and without applying PFG and  $\gamma$  is the gyromagnetic ratio ( $\text{rad}, \text{T}^{-1}, \text{s}^{-1}$ ). During these experiments, the strength of PFG (variable  $g$  in Eq. 1) was increased in a successive manner, while all the other parameters were kept constant.  $D_T$  can then be derived from the slope of the linear plot of  $\ln(A')$  versus  $g^2$ . Precautions were taken to ensure the accurate measurement of  $D_T$ . This included selecting a range of gradient field strength to clearly observe signal intensity modulation. In our reported experiments, the higher  $\Delta x(\delta g)^2/10^6$  values used were up to 46, resulting in a greater than 90% change in spin echo amplitudes or signal intensities.

The gradient field strength was calibrated using a gradient echo pulse with a 60%  $\text{H}_2\text{O}/40\%$   $\text{D}_2\text{O}$  sample in a matched Shigemi tube. Data points were acquired with gradient on. The length of the sample varied as 4, 7 and 10 mm, while the gradient strength was changed from 10% to 30%. Gradient field strength  $g$  (G/cm) equals  $\Delta\nu \times 10^{-3}/(\Delta x \times 4.258)$ , where  $\Delta\nu$  is the linewidth of the  $\text{H}_2\text{O}$  signal in Hz and  $\Delta x$  is the sample length in cm. A full-range (5–99% of total gradient strength) calibration was

conducted using the lysozyme sample and experimental parameters comparable to those reported in the literature (Altieri et al., 1995; Ilyina et al., 1997) and also those used for oligonucleotide experiments. Using the known  $D_T$  value ( $11.0 \times 10^{-7} \text{ cm}^2/\text{s}$  at 298 K; Ilyina et al., 1997), the actual gradient strength was backcalculated and a linear correction function ( $g(\text{actual}) = ag(\text{experimental}) + b$ , where  $a$  and  $b$  are constants and are 0.628 and 4.586, respectively) was derived by data fitting in the 35–99% range. This effectively also calibrated the gradient amplitude due to the discrepancy between the rectangular gradient pulses cited in the literature (Gibbs and Johnson, 1991) and the sine-shaped pulses used in our experiments. These calibrated gradient strength values were used in deriving the  $D_T$  of oligonucleotides.

NMR data were processed using the UXNMR (Bruker Instruments Inc.) and the FELIX v. 950 (Molecular Simulations Inc.) programs. Signal intensities,  $A'$ , of several resonances were monitored for each of the sequences (Figs. S2 and S3, supplementary material). A typical set of experimental spectra for d1s is displayed in Fig. 3, in which three resonances at 8.00, 6.04 and 1.74 ppm for G2 H8, G4 H1' and T7 5-methyl protons are shown to decay according to Eq. 1. To derive  $D_T$ , the selected peak intensities,  $\ln(A')$ , were plotted against  $g^2$  to give linear lines as illustrated in Fig. 4 (note that the  $g$  values in the figure are uncorrected spectrometer settings). After applying the  $g$  correction, the least-squares fitting of these linear lines produced their slope values, from which  $D_T$  values for each of the marked resonances were calculated ( $D_T = -\text{slope}/((\gamma\delta)^2(\Delta - \delta/3))$ ). The  $D_T$  data for the three single strands and the two duplexes are summarized in Table 1. These are mean values and respective root-mean standard deviations (rmsd) derived from three data sets for each of the five sequences.

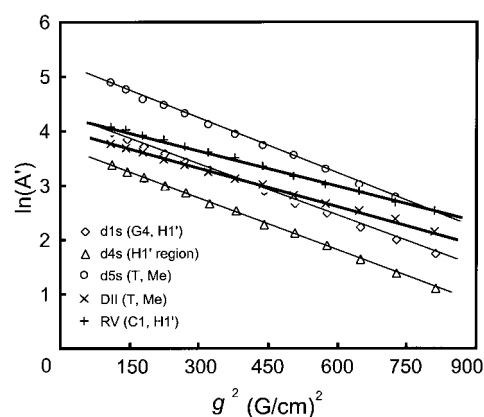


Fig. 4. Representative  $^1\text{H}$  signal intensity ( $\ln(A')$ ) as a function of gradient field strength  $g^2$  ( $\text{G}/\text{cm})^2$  ( $g$  is the experimental rather than corrected gradient strength). One data set was chosen for each of the molecules measured. Diffusion constants were calculated according to Eq. 1 (note that the actual field strength was calibrated as described in the Materials and Methods section). The two heavier lines show linear plots of the DII and RV duplexes.

## Results and Discussion

Our measurements of  $D_T$  involved three DNA single strands (the unmodified d1s and the backbone modified d4s and d5s) in comparison with two related duplexes – the hybrid RV duplex (d5s and the complementary RNA strand) and the modified DNA duplex DII (Fig. 1). The conformations of these sequences have been investigated by temperature-dependent 1D and 2D NMR and UV experiments (Yang et al., manuscript in preparation). These studies demonstrate that at 300 K, d1s (the natural DNA oligonucleotide strand) and d5s (containing two alternating MMI backbone linkers) form stable structures, while d4s (containing a single MMI modified backbone linkage) does not appear to be structured as judged from the absence of base paired imino and amino  $^1\text{H}$  resonances (Fig. S1, supplementary material). At this temperature, both RV and DII are stable duplexes (the  $T_m$  values of the two duplexes by UV are 325.2 and 326.7 K, respectively). In this experiment, the question of whether d1s and d5s form hairpins or homo-duplexes was investigated. The typical PFG  $D_T$  experimental spectra and data analysis under the given salt, pH and solvent conditions (see also the Materials and Methods section) are illustrated in Figs. 3 and 4 and the  $D_T$  values are summarized in Table 1. It is noted that the  $D_T$  values reported here compare reasonably well with those for an 8-mer ( $d(\text{CG})_4$ ,  $D_T = 16.5 \times 10^{-7} \text{ cm}^2/\text{s}$ ), a 12-mer ( $d(\text{CG})_6$ ,  $D_T = 14.6 \times 10^{-7} \text{ cm}^2/\text{s}$ ) and a 20-mer sequence ( $d(\text{CGTACTGTAACTAGTACG})$ ,  $D_T = 12.1 \times 10^{-7} \text{ cm}^2/\text{s}$ ) measured by depolarized dynamic light scattering at a concentration of 10 mg/ml, at 298 K (Eimer and Pecora, 1991).

The results of the  $D_T$  measurements at 300 K, in combination with UV and NMR studies (Yang et al., manuscript in preparation), clearly indicate that at this temperature d1s and d5s remain as hairpins.  $D_T$  is influenced by various factors, such as temperature and frictional forces (recall the Einstein equation,  $D_T = k_b T/f$ , where  $f$  is the frictional coefficient ( $= 6\pi\eta r$ , where  $\eta$  is the viscosity)) as described in a number of hydrodynamic models (Tirado and Garcia de la Torre, 1979,1980; Teller et al., 1979; Cantor and Schimmel, 1980). Several other factors also contribute to  $D_T$ , such as roughness of the surface, surface polarity, etc. (for a discussion, see Tinoco et al. (1995)). When the effects of molecular mass, size, shape and flexibility on  $f$  are considered, the empirical relationship exists

as  $f \propto M^\lambda$ , and the value of  $\lambda$  is between 0.33 and 0.8, depending on the properties of molecules (Cantor and Schimmel, 1980). For a rigid spherical molecule,  $\lambda = 0.33$  and this value increases when structures become more flexible and/or molecular shapes are more rod-like than spherical.  $D_T$ , therefore, is proportional to  $M^{-\lambda}$ . Following these relationships, the dimerization of a globular protein was found to give a  $D_{T,\text{monomer}}/D_{T,\text{dimer}} \sim 1.4$ , which correlates to  $\lambda = 0.5$  or  $D_T \propto M^{-0.5}$  (Altieri et al., 1995; Lin and Larive, 1995; Ilyina et al., 1997). A molecule in a random single-stranded (ss) conformation is more flexible and is, thus, expected to diffuse at a rate slower than that of a hairpin. Therefore,  $D_{T,\text{ss}}$  should be smaller than  $D_{T,\text{hairpin}}$ . A smaller ratio ( $\sim 1.14$ – $1.19$ ) between the  $D_T$ 's of a dodecamer hairpin and a duplex was calculated from the symmetrical cylinder models (Tirado and Garcia de la Torre, 1979,1980; Eimer and Pecora, 1991). In our experiment, the  $D_T$  values of the two structured, single stranded sequences, d1s and d5s, were measured at  $13.6 \times 10^{-7}$  and  $14.8 \times 10^{-7} \text{ cm}^2/\text{s}$ , respectively. These results are compared with those of the RV and DII duplexes to give a ratio of  $\sim 1.40$  (Table 1). These ratios agree well with that expected for  $D_{T,\text{hairpin}}/D_{T,\text{duplex}}$ , based on  $D_T \propto M^{-0.5}$  and the protein dimerization data (Altieri et al., 1995; Lin and Larive, 1995; Ilyina et al., 1997), thus ruling out the formation of  $(d1s)_2$  or  $(d5s)_2$  homo-duplexes (Fig. 2), which would give  $D_T$  values similar to those of DII and RV. Based on this result, we have been able to initiate the computational effort to evaluate the conformations of loop residues in d1s and d5s, which will provide insights into the structural functions of chemically modified backbone linkers. The measured  $D_T$  value for single-stranded d4s is comparable to d1s or d5s, implying that their overall shapes are likely to be similar. This suggests that even though the base paired  $^1\text{H}$  resonances of d4s were not detectable, this sequence does not appear to assume a completely, randomly coiled conformation but it may be locally structured. Taking the NMR results together, it indicates that the absence of stable imino proton resonances in d4s is likely due to conformational exchanges and/or fast exchange of these protons with solvent. These possibilities are not further differentiated in the PFG experiment, which measures statistically averaged  $D_T$  values, if individual conformations do not display a resolved signal. The PFG NMR has thus provided information on the conformational states of oligonucleotides which would

TABLE 1  
DIFFUSION CONSTANTS FOR OLIGONUCLEOTIDES<sup>a</sup>

d1s	d4s	d5s	DII	RV
$13.6 \pm 0.3^b$	$14.0 \pm 0.1$	$14.8 \pm 0.1$	$9.9 \pm 0.0$	$10.0 \pm 0.0$
$0.9983 \pm 0.0003^c$	$0.9964 \pm 0.0010$	$0.9960 \pm 0.0012$	$0.9947 \pm 0.0011$	$0.9925 \pm 0.0049$

<sup>a</sup> Diffusion constants measured at 300 K are reported in units of  $\times 10^7 \text{ cm}^2/\text{s}$ .

<sup>b</sup> Mean values and standard deviations from three experimental data sets.

<sup>c</sup> Correlation coefficient for the linear line fitting.

not be available from the conventional exchangeable proton experiments.

## Conclusions

A simple experiment was described for the measurements of the diffusion constants of a set of oligonucleotides, which are comparable in sequence composition and chain length but differ in backbone chemical structure. The results of these experiments provide direct assessment of the polymeric and conformational states of oligonucleotides under NMR conditions. These results, in combination with conventional NMR spectral analysis, allow for the confirmation of hairpin formation by the single-stranded d1s and d5s. This conclusion was otherwise ambiguous due to the spectral similarity between the hairpin and the homo-duplex forms. The PFG experiments also identify the potential existence of the structured, single-stranded conformations, which do not show hydrogen bonded imino proton resonances. The unambiguous assignments of the strand folding of the single-stranded oligonucleotides with or without backbone modifications reveal the important role of the backbone linkers in the formation of single-stranded structures and in determining their conformational flexibilities. This information should help us better understand the biological effect of the various antisense sequences.

## Acknowledgements

This research was supported by NIH (R29 GM49957-01) and the Robert A. Welch Foundation (E-1270). The 600 MHz NMR spectrometer at the University of Houston was funded by the W.M. Keck Foundation. The authors thank Minxue Zheng for help with the PFG experiments and Robert Taylor (Bruker Instruments) for technical help. The formacetal and the 3'-thioformacetal backbone modified sequences were generous gifts from Gilead Sciences and Glaxo Pharmaceuticals Inc.

## References

- Agrawal, S. and Iyer, R.P. (1995) *Curr. Opin. Biotechnol.*, **6**, 12–19.
- Altieri, A.S., Hinton, D.P. and Byrd, R.A. (1995) *J. Am. Chem. Soc.*, **117**, 7566–7567.
- Antalek, B. and Windig, W. (1996) *J. Am. Chem. Soc.*, **118**, 10331–10332.
- Barjat, H., Morris, G., Smart, S., Swanson, A.G. and Williams, C.R. (1995) *J. Magn. Reson.*, **108**, 170–172.
- Bax, A., De Jong, P.G., Mehlkopf, A.F. and Smidt, J. (1980) *Chem. Phys. Lett.*, **69**, 567–570.
- Cantor, C.R. and Schimmel, P.R. (1980) *Biophysical Chemistry*, Part III, Freeman, New York, NY, U.S.A., pp. 979–1001; 1019–1040.
- Carr, H.Y. and Purcell, E.M. (1954) *Phys. Rev.*, **94**, 630–638.
- Chattopadhyaya, R., Grzeskowiak, K. and Dickerson, R.E. (1990) *J. Mol. Biol.*, **211**, 189–210.
- Cole-Strauss, A., Yoon, K., Xiang, Y., Byrne, B.C., Rice, M.C., Gryn, J., Holloman, W.K. and Kmiec, E.B. (1996) *Science*, **273**, 1386–1389.
- Crooke, S.T. (1992) *Annu. Rev. Pharmacol. Toxicol.*, **32**, 329–376.
- Cross, C., Rice, J.S. and Gao, X. (1997) *Biochemistry*, **36**, 4096–4107.
- Eimer, W., Williamson, J.R., Boxer, S.G. and Pecora, R. (1990) *Biochemistry*, **29**, 799–811.
- Eimer, W. and Pecora, R. (1991) *J. Chem. Phys.*, **94**, 2324–2329.
- Gao, X., Brown, F.K., Jeffs, P., Bischofberger, N., Lin, K.-Y., Pipe, A.J. and Noble, S.A. (1992) *Biochemistry*, **31**, 6228–6236.
- Gao, X. and Jeffs, P.W. (1994a) *J. Biomol. NMR*, **4**, 17–34.
- Gao, X. and Jeffs, P.W. (1994b) *J. Biomol. NMR*, **4**, 367–384.
- Gibbs, S.J. and Johnson Jr., C.S. (1991) *J. Magn. Reson.*, **93**, 395–402.
- Gozansky, E. and Gorenstein, D.G. (1996) *J. Magn. Reson.*, **B111**, 94–96.
- Hahn, E.L. (1950) *Phys. Rev.*, **80**, 580–594.
- Harris, R.K. (1986) *Nuclear Magnetic Resonance Spectroscopy*, Longman Scientific & Technical, London, U.K., pp. 81–84.
- Hilbers, C.W., Haasnoot, C.A., De Bruin, S.H., Joordens, J.J., Van der Marel, G.A. and Van Boom, J.H. (1985) *Biochimie*, **67**, 685–695.
- Hurd, R.E. (1990) *J. Magn. Reson.*, **87**, 422–428.
- Ilyina, E., Roongta, V., Pan, H., Woodward, C. and Mayo, K. (1997) *Biochemistry*, **36**, 3383–3388.
- Ippel, J.H., Lanzotti, V., Galeone, A., Mayol, L., Van den Boogaart, J.E., Pikkemaat, J.A. and Altona, C. (1995) *Biopolymers*, **36**, 681–694.
- Kay, L.E., Keifer, P. and Saarinen, T. (1992) *J. Am. Chem. Soc.*, **114**, 10663–10665.
- Lin, M. and Larive, C.K. (1995) *Anal. Biochem.*, **229**, 214–220.
- Matteucci, M.D. and Wagner, R.W. (1996) *Nature*, **384** (Suppl.), 20–22.
- McCain, D.C. (1995) *J. Magn. Reson.*, **B109**, 209–212.
- Patel, D.J., Shapiro, L. and Hare, D. (1987) *Q. Rev. Biophys.*, **20**, 35–112.
- Rice, J.S. and Gao, X. (1997) *Biochemistry*, **36**, 399–411.
- Ruiz-Cabello, J., Vuister, G.W., Moonen, C.T.W., Van Gelderen, P., Cohen, J.S. and Van Zijl, P.C.M. (1992) *J. Magn. Reson.*, **100**, 282–302.
- Sanghvi, Y.S. (1997) In *Comprehensive Natural Products Chemistry*, Vol. 7: *DNA and Aspects of Molecular Biology* (Eds., Barton, D.H.R. and Nakanishi, K.), Pergamon, in press.
- Sendhil, S. and Chandrakumar, N. (1996) *J. Magn. Reson.*, **A123**, 122–125.
- Senior, M.M., Jones, R.A. and Breslauer, K.J. (1986) *Proc. Natl. Acad. Sci. USA*, **85**, 6242–6246.
- Stein, C.A. (1996) *Chem. Biol.*, **3**, 319–323.
- Stejskal, E.O. and Tanner, J.E. (1965) *J. Chem. Phys.*, **42**, 288–292.
- Tanner, J.E. (1970) *J. Chem. Phys.*, **52**, 2523–2526.
- Teller, D.C., Swanson, E. and De Haen, C. (1979) *Methods Enzymol.*, **61**, 103–124.
- Tinoco Jr., I., Sauer, K. and Wang, J.C. (1995) *Physical Chemistry Principles and Applications in Biological Sciences*, 3rd ed., Prentice-Hall, Englewood Cliffs, NJ, U.S.A., pp. 268–295.
- Tirado, M.M. and Garcia de la Torre, J. (1979) *J. Chem. Phys.*, **71**, 2581–2587.
- Tirado, M.M. and Garcia de la Torre, J. (1980) *J. Chem. Phys.*, **73**, 1986–1993.
- Varani, G. (1995) *Annu. Rev. Biophys. Biomol. Struct.*, **24**, 379–404.
- Vasseur, J.J., Debart, F., Sanghvi, Y.S. and Cook, P.D. (1992) *J. Am. Chem. Soc.*, **114**, 4006–4007.
- Veal, J.M., Gao, X. and Brown, F.K. (1993) *J. Am. Chem. Soc.*, **115**, 7139–7145.
- Veal, J.M. and Brown, F.K. (1995) *J. Am. Chem. Soc.*, **117**, 1873–1880.
- Vesnaver, G. and Breslauer, K.J. (1991) *Proc. Natl. Acad. Sci. USA*, **88**, 3569–3573.
- Williamson, J.R. and Boxer, S.G. (1989a) *Biochemistry*, **28**, 2819–2831.
- Williamson, J.R. and Boxer, S.G. (1989b) *Biochemistry*, **28**, 2831–2836.
- Zamecnik, P.C. and Stephenson, M.L. (1978) *Proc. Natl. Acad. Sci. USA*, **75**, 280–284.